PRAMANA
— journal of
physics

Vol. 57, No. 4
October 2001
pp. 733–741

Scattering and absorption differential cross sections for double photon Compton scattering

B S SANDHU*, M B SADDI, B SINGH and B S GHUMMAN
Physics Department, Punjabi University, Patiala 147 002, India
*Author for correspondence

MS received 28 August 2000

Abstract. The scattering and absorption differential cross sections for nonlinear QED process such as double photon Compton scattering have been measured as a function of independent final photon energy. The incident gamma photons are of 0.662 MeV in energy as produced by an 8 Ci ^{137}Cs radioactive source and thin aluminum foils are used as scatterer. The two simultaneously emitted photons in this process are detected in coincidence using two NaI(T1) scintillation detectors and a slow-fast coincidence set-up of 30 nsec resolving time. The measured values of scattering and absorption differential cross sections agree with theory within experimental estimated error.

Keywords. Double photon Compton scattering; scattering and absorption cross sections; coincidence spectra; coincidence events.

PACS Nos 13.60.-r; 13.60.Fz; 32.80.-t; 32.80.Wr; 32.80.Cy

1. Introduction

In the collision between a photon and a free electron, quantum electrodynamics predicts the existence of higher order processes, in addition to single (or normal) photon Compton scattering. These higher order processes are typical quantum effects and most significant among these is double photon Compton scattering, in which the collision products are two degraded gamma quanta at the same time as the recoil electron. An exact theory of this effect is provided by Mandl and Skyrme [1] using *S*-matrix formalism of quantum electrodynamics. Their expression for the collision differential cross section can be regarded as double photon Compton analog of the well-known Klein–Nishina relation for single photon Compton scattering. They also simplified the expression for collision differential cross section in a number of several experimentally realizable cases.

This nonlinear phenomenon is important because it provides a test of quantum electrodynamics implicitly, a mechanism of photon multiplication along with the bremsstrahlung in astrophysics, a major background process in the experimental study of another nonlinear QED process namely photon splitting in electric fields of heavy atoms and there is appreciable contribution of this process to total scattering coefficients at extremely higher energies where this phenomenon is more likely to occur.

Measurements confirming the existence of this higher order process have been given in a previous paper [2] to which we refer for literature on the theoretical studies on this process and on preceding experimental results. The limitations suffered by the various measurements reported in the literature are also mentioned therein. Our previous measurements [2–4] are confined to energy, angular distribution, collision differential cross section and collision cross section integrated over energy, and confirm some elementary features of the theory of double photon Compton effect.

The scattering and absorption differential cross sections for single photon Compton scattering are described in detail by Evans [5], but no data are available for these cross sections in the case of double photon Compton scattering. In the present work, of academic interest, these cross sections are measured as a function of independent final photon energy for 0.662 MeV incident gamma photons. The two simultaneously emitted gamma quanta are detected at $\theta_1 = \theta_2 = \pi/2$ and the angle between them being $3\pi/4$. This particular geometry corresponds to simple experimentally realizable case and thus provides data for these scattering and absorption cross sections.

2. Experimental set-up

The experimental arrangement used for the present measurements is shown in figure 1, in which an intense beam of gamma rays from 8 Ci (1 Ci = 37 Gbq) ^{137}Cs radioactive source is made to impinge on an aluminium scatterer. The cylindrical beam collimator consisting of a brass pipe and fitted with aluminium windows on both the ends can be filled with a column of mercury when desired and is used to close the incident beam. The conical lead collimator reduces the effect of scattering from the edges. The two simultaneously emitted gamma quanta in this process are detected by two NaI(Tl) scintillation detectors D_1 (in the direction θ_1) and D_2 (in the direction θ_2, ϕ_2) having dimensions 51 $\times$ 51 mm and 45 $\times$ 25 mm respectively. The scattering plane is defined by S-Sc-D_1. The detector assemblies are arranged in such a way that the axes of two gamma detectors and the source collimator pass through the centre of scatterer. Both the detectors are properly shielded by cylindrical lead shielding and the inner side of each shielding is covered with 2 mm thick iron and 1 mm thick aluminium, with iron facing lead to absorb K x-rays emitted by lead shielding. The faces of both the detectors are also placed well inside the cylindrical lead shielding to prevent the photons scattered from face of one detector from reaching the other. The positions of the two detectors are adjusted in such a way that they do not view the source window directly. For the present measurements the angular spread due to detector apertures are 8.3° and 11.9° respectively. The timing electronics using Canberra ARC timing amplifiers and of 30 nsec resolving time is used to record these events. It is determined that fast coincidence efficiency is nearly 100% for gamma ray energies larger than 25 keV if the resolving time is set at a nominal value of 30 nsec.

The photopeak efficiency curves for both the detectors are shown in figure 2. These curves are obtained from data for intrinsic efficiency and photofraction reported by Crouthamel [6], and corrected for iodine escape peak [7,8] and absorption in aluminium windows [9]. The experimental measured values of photopeak efficiency of both the detectors using single energy sources of ^{137}Cs and ^{203}Hg of known source strengths are found to be nearly in agreement with theoretical values.

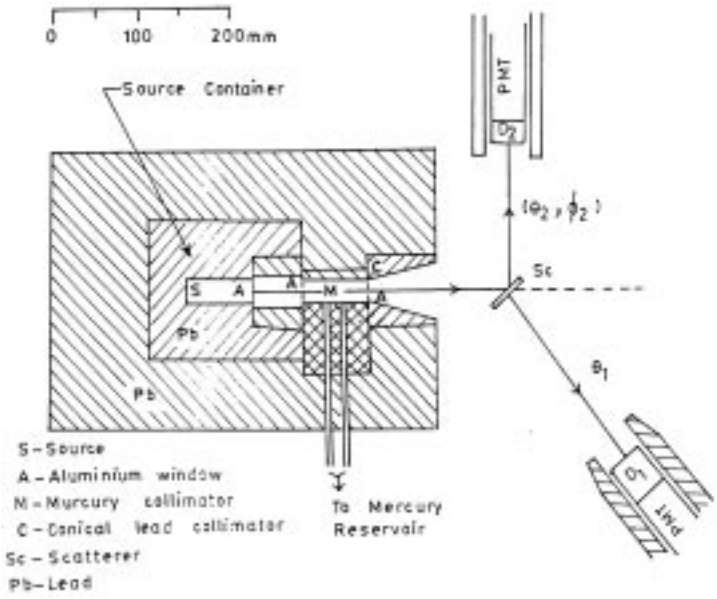

Figure 1. Experimental set-up, S: 8 Ci ^{137}Cs radioactive source; Sc: aluminium scatterer; D_1, D_2: NaI(T1) scintillation detectors; Pb: lead shielding.

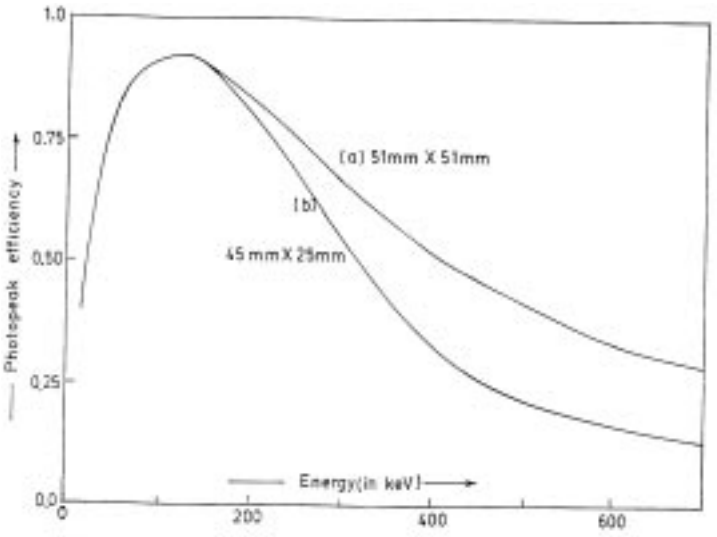

Figure 2. Photopeak efficiency of NaI(Tl) gamma detector, (a) 51 $\times$ 51 mm and (b) 45 $\times$ 25 mm.

3. Method of measurements

The scattering and absorption cross sections are to be distinguished clearly from collision cross section. The collision cross sections refer to the number of collisions of any particular type, and they describe the number of photons which are scattered in a particular direction, as a fraction of the number of incident photons. In sharp contrast, Compton scattering cross sections refer to the amount of energy scattered in a particular direction, and they describe the energy content of the photons which are scattered in a particular direction, as a fraction of the incident intensity. The scattering differential cross section, $(\mathrm{d}^3\sigma/\mathrm{d}\Omega_1\mathrm{d}\Omega_2\mathrm{d}E_2)_{\text{scattering}}$ or in short as $\mathrm{d}({}_e\sigma_s)$, representing scattering or mere deflection of electromagnetic radiation (gamma rays) is given by the relation:

$$\mathrm{d}({}_e\sigma_s) = (N_d/N_s)\{(E_1+E_2)/E_0\}\langle \mathrm{d}\sigma_{\mathrm{KN}}/\mathrm{d}\Omega_1\rangle \varepsilon'(E')/\{\varepsilon_1(E_1)\Omega_2\varepsilon_2(E_2)\}, \tag{1}$$

where N_d is the coincidence count rate per unit energy interval due to double photon Compton scattering events; N_s is the single photon Compton scattering count rate for the detector D_1; Ω_1 and Ω_2 are solid angles subtended by the two detectors at the scattering centre; $\langle \mathrm{d}\sigma_{\mathrm{KN}}/\mathrm{d}\Omega_1\rangle$ is the Klein–Nishina cross section for single photon Compton scattering in the direction of detector D_1 and averaged over the subtended solid angle; E_0 being the incident photon energy; $\varepsilon_1(E_1)$ and $\varepsilon_2(E_2)$ are the efficiencies of the two detectors for two emitted gamma photons having energies E_1 and E_2 respectively; and $\varepsilon'(E')$ is the efficiency of the detector D_1 corresponding to energy E' due to single photon Compton scattering in the direction of the detector.

In a similar way the absorption differential cross section, $(\mathrm{d}^3\sigma/\mathrm{d}\Omega_1\mathrm{d}\Omega_2\mathrm{d}E_2)_{\text{absorption}}$ or in short as $\mathrm{d}({}_e\sigma_a)$, representing true absorption of energy from the electromagnetic radiation is given by the relation:

$$\mathrm{d}({}_e\sigma_a) = (N_d/N_s)\{1-(E_1+E_2)/E_0\}\langle \mathrm{d}\sigma_{\mathrm{KN}}/\mathrm{d}\Omega_1\rangle \varepsilon'(E')/\{\varepsilon_1(E_1)\Omega_2\varepsilon_2(E_2)\}. \tag{2}$$

Since the collision differential cross section, $(\mathrm{d}^3\sigma/\mathrm{d}\Omega_1\mathrm{d}\Omega_2\mathrm{d}E_2)_{\text{collision}}$ or in short as $\mathrm{d}({}_e\sigma)$, for this process varies over the finite energy spread (25 keV for the present measurements); the independent energy levels of the second photon are evaluated as average of the energy values weighted in proportion to the probability for occurrence of this process according to the following relation:

$$E_2 = \left[\int_{\Delta E_2} E_2\{\mathrm{d}({}_e\sigma(E_2))\}\mathrm{d}E_2\right] \Big/ \left[\int_{\Delta E_2} \{\mathrm{d}({}_e\sigma(E_2))\}\mathrm{d}E_2\right], \tag{3}$$

where ΔE_2 being the energy window of second photon detected by detector D_2.

The quantities such as N_d, N_s and E_1 are measured experimentally. The solid angles are measured from the geometry of the experimental set-up. Independent energy levels of second photon having energy E_2 are evaluated using eq. (3). Single photon Compton cross sections are calculated from the Klein–Nishina relation and detector efficiencies are evaluated from the curves of figure 2.

In the present measurements, we have recorded the coincidence spectrum of one of the emitted photons, E_1, by fixing the energy window of the second photon, E_2, on ND62

MCA, which is gated with the output of the coincidence set-up. Both the detectors are biased above the K x-ray energy of the scatterer (1.56 keV for aluminum scatterer). Seven different energy intervals of E_2 have been selected and the corresponding energy spectra of E_1 are recorded. An energy spread of 25 keV is selected to achieve a reasonable coincidence count rate. The coincidence count rates are recorded with and without aluminium scatterer in the primary incident gamma beam. The chance coincidence count rates in these measurements are also recorded by introducing a suitable delay in one of the detecting channels. The single photon Compton scattered spectrum for one of the detectors D_1 is recorded with the same aluminium scatterer in the primary beam. The true coincidence spectrum due to double photon Compton scattering events is obtained by subtracting the contribution of target-out and chance coincidences from the observed target in coincidences. As the probability of occurrence of this process is quite small, the experiment is run over a long period of time to achieve a reasonable counting statistics. The calibration and stability of the system are checked regularly and adjustment are made if required.

4. Results and discussion

A typical coincidence spectrum, corrected for coincidences unrelated to the target and chance events, of one of the emitted photon's for a fixed energy window of the second photon is shown in figure 3. The error bars represent statistical uncertainties and the solid curve represents the best-fit curve through the experimental points corresponding to the peak observed in the energy spectrum and the measured values of energy corresponding to the peaks observed in energy spectra for different energy windows of the second photon having energy E_2 are given in column 3 of table 1. It has been seen that the shift in energy corresponding to the peaks observed in the energy spectra for different target thicknesses is within experimental estimated error of nearly 3%. The independent energy levels of the second photon, evaluated as average of the energy values weighted in proportion to the probability for occurrence of this process according to eq. (3), are given in column 2 of table 1.

The observed coincidence count rate per unit energy interval under the peak of the recorded coincidence spectrum consists of coincidences resulting from interaction in the target. These coincidences correspond to double photon Compton (DPC) scattering and Compton–bremsstrahlung (CB) events. A CB event results from the detection of bremsstrahlung produced by the recoil Compton electron in coincidence with the single photon Compton scattered gamma ray. A theoretical calculation of the CB events is rendered uncertain by scattering of the recoil electron before emission of bremsstrahlung, so an experimental approach suggested by Cavanagh [10] is used to eliminate CB events. The DPC count rate varies linearly and the CB count rate quadratically with target thickness. The energy spectra are thus recorded with four different target thicknesses of 13, 27.5, 40 and 53.5 mg-cm^{-2}. A plot of coincidence count rate per unit thickness versus thickness for such a series would be a straight line of positive slope if CB background is significant and such a plot is shown in figure 4. The error bars represent statistical errors only and the straight line represents a least-squares fit to the data. The CB background is eliminated by extrapolating the coincidence count rate to unit thickness. The CB background amounts on the average to about 11% of the DPC count rate for thickest target.

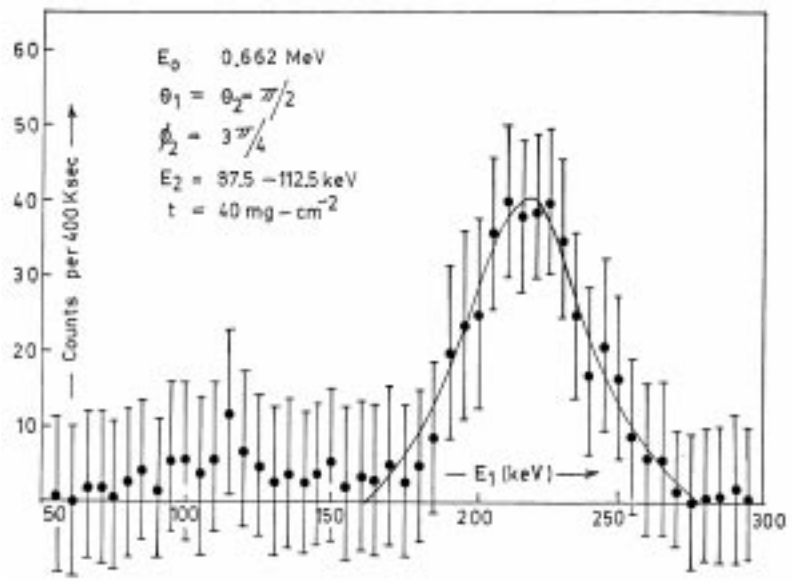

Figure 3. Energy distribution of E_1 for $E_2 = 87.5$–112.5 keV. The error bars represent statistical uncertainties only.

Table 1. Present measured values of scattering and absorption differential cross sections of double photon Compton scattering for 0.662 MeV incident gamma photons at $\theta_1 = \theta_2 = \pi/2$ and $\phi_2 = 3\pi/4$. The errors represent statistical uncertainties only.

			Differential cross section ($\times 10^{-32}$ cm^2 sr^{-2} keV^{-1})			
			$d(_e\sigma_s)$		$d(_e\sigma_a)$	
ΔE_2 (in keV)	E_2 (in keV)	E_1^{Exptl} (in keV)	Exptl.	Theory	Exptl.	Theory
62.5–87.5	73.8	251.0	1.59 ± 0.12	1.58	1.70 ± 0.13	1.75
87.5–112.5	99.0	218.0	0.95 ± 0.11	0.98	1.04 ± 0.13	1.05
112.5–137.5	124.3	205.0	0.17 ± 0.12	0.67	0.71 ± 0.12	0.70
137.5–162.5	149.6	172.0	0.52 ± 0.06	0.53	0.55 ± 0.06	0.54
162.5–187.5	175.1	153.0	0.49 ± 0.06	0.50	0.50 ± 0.06	0.51
187.5–212.5	200.6	126.5	0.61 ± 0.07	0.59	0.62 ± 0.08	0.61
212.5–237.5	226.1	94.0	0.87 ± 0.10	0.85	0.93 ± 0.10	0.91

The scattering and absorption differential cross sections for double photon Compton scattering, for different energy intervals of second photon having energy window ΔE_2, are calculated from coincidence count rate due to DPC scattering, single photon Compton scattering count rate and other required parameters. The measured values of the scattering and absorption differential cross sections are given in columns 4 and 6 respectively of table 1. Columns 5 and 7 give the corresponding values calculated from eqs (A3) and (A8) respectively of Appendix-A for the same energy and direction of emission of scattered photons. The errors indicate statistical uncertainties only. The measured values of scattering and absorption differential cross sections are also shown in figure 5.

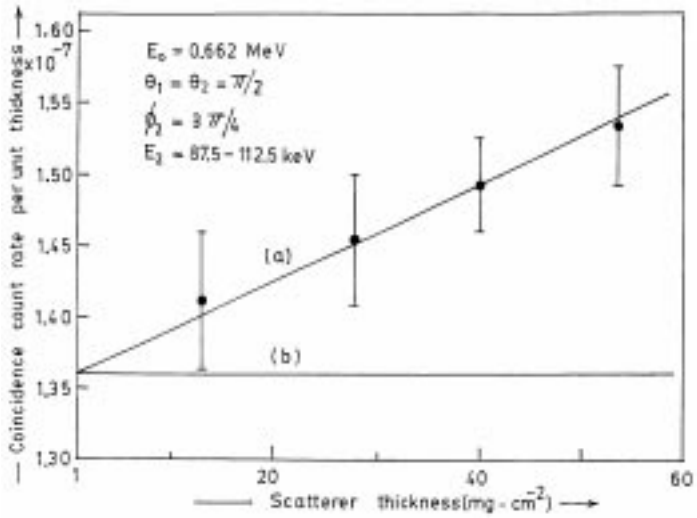

Figure 4. Coincidence count rate per unit thickness versus target thickness. Curve (a) – coincidences due to DPC and CB events. Curve (b) – coincidences due to DPC events. The error bars represent statistical error only.

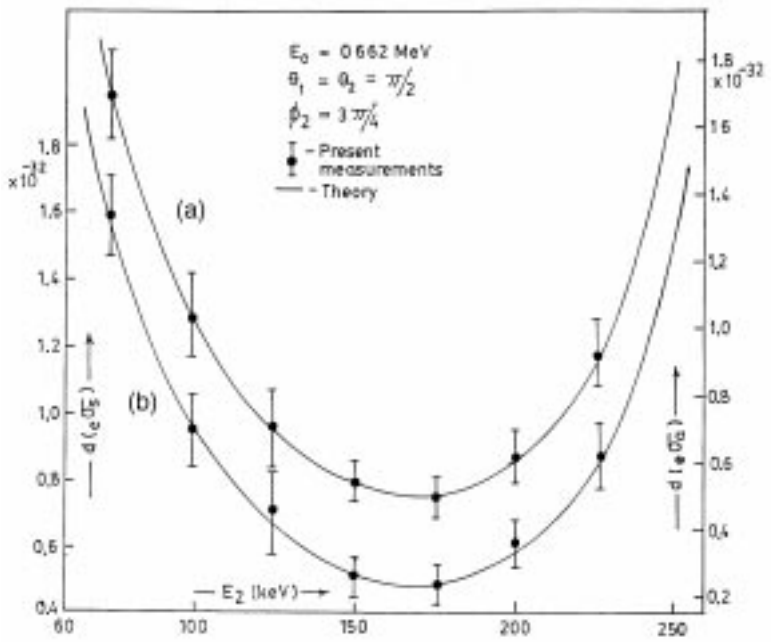

Figure 5. The scattering (curve (a), scale along left Y-axis) and absorption (curve (b), scale along right Y-axis) differential cross sections as function of independent final photon energy for 0.662 MeV incident gamma photons at $\theta_1 = \theta_2 = \pi/2$, and $\phi_2 = 3\pi/4$.

The errors in the present measurements of the differential cross section are due to statistical uncertainties in the coincidence count rate due to DPC events (∼10–15%), single photon Compton scattering count rate (∼0.8%), solid angles (∼1.5%), scatterer thickness (∼0.5%) and detector efficiencies (∼5%). The maximum uncertainty in the measurement of energy is estimated to be less than 3%. The self absorption in the scatterer is estimated to be less than 0.8%. The probabilities of photons being split by the nuclear electrostatic field [11] and detector to detector scattering contribution to coincidences is almost negligible. The contribution to coincidences due to higher order process like triple photon Compton scattering is also negligible, as the cross section for this process is α (find structure constant) times the value for double photon Compton scattering. Our measured results for scattering and absorption differential cross sections are in agreement with theory within experimental estimated error of nearly 25%.

Our results of double photon Compton scattering support the theoretical scattering and absorption differential cross section formulae for this higher order process. Nevertheless the understanding of these partial cross sections in this phenomenon is certainly incomplete. No doubt the experiment requires long period of exceptional stability, because the coincidence count rates are too small, the future experiments must be performed at small scattering angles and higher incident photon energies where this nonlinear QED process is more likely to occur. It is further planned to perform more measurements on this process in the forward hemisphere using HPGe detector since the present data suffer from poor energy resolution of scintillation spectrometers.

Appendix A

The energy E_1 of one of the emitted photon in terms of E_0, E_2 (energy of the other photon) and scattering angles, using the conservation of energy and momenta, is given by

$$E_1 = [m_0c^2\{E_0 - E_2(1+G)\}]/[m_0c^2 + E_0(1-\cos\theta_1) - E_2(1-\cos\theta_{12})] \tag{A1}$$

with $G = \{E_0/(m_0c^2)\}(1-\cos\theta_2)$, the angles θ_1 and (θ_2, ϕ_2) define direction of emission of the two emitted photons having energies E_1 and E_2 respectively and θ_{12} being angle between momentum vectors of the two emitted photons in this process is given by

$$\cos\theta_{12} = \cos\theta_1\cos\theta_2 + \sin\theta_1\sin\theta_2\cos\phi_2. \tag{A2}$$

The expression for the scattering differential cross section, $\mathrm{d}({}_e\sigma_s)$, representing scattering or mere deflection of electromagnetic radiation (gamma rays) is given by the relation:

$$\mathrm{d}({}_e\sigma_s) = (\alpha r_0^2/16\pi^2 m_0c^2)(E_1E_2/E_0)(X/T_s). \tag{A3}$$

In this expression α is the fine structure constant, $r_0 (= e^2/m_0c^2)$ is the classical electron radius, E_0 being the incident photon energy, E_1 and E_2 are the energies of the emitted photons, with E_2 regarded as independent final photon energy. T_s and X are complicated functions of energies and scattering angles of the photons given as

$$T_s = (k_0/(k_1+k_2))\{1 + k_0(1-\cos\theta_2) - k_1(1-\cos\theta_{12})\}, \tag{A4}$$

$$\begin{aligned} X &= -2(\alpha\beta-\gamma)^2+4(\alpha\beta-\gamma)(\alpha+\beta)-16\alpha\beta+8\gamma-2\xi(\alpha^2+\beta^2) \\ &\quad +2(\alpha\beta-\gamma)\xi(\alpha+\beta)-4\xi(\eta\zeta)^{-1}[\xi^2(\delta-1)-2\delta] \\ &\quad\quad +4\xi(\xi+1)(\eta^{-1}+\zeta^{-1}) \\ &\quad -4[2\xi+\delta(1-\xi)](\alpha\zeta^{-1}+\beta\eta^{-1})-2[\alpha\beta+\gamma(1-\xi)]\rho, \end{aligned} \tag{A5}$$

where $\alpha, \beta, \ldots$ are defined in terms of the a_i and b_i by

$$\begin{aligned} &\alpha=\Sigma a_i^{-1},\ \beta=\Sigma b_i^{-1},\ \gamma=\Sigma(a_i\,b_i)^{-1},\ \eta=a_1a_2a_3,\ \zeta=b_1b_2b_3, \\ &\delta=\Sigma a_ib_i,\ \rho=\Sigma(a_i/b_i+b_i/a_i),\ \xi=\Sigma a_i=\Sigma b_i \end{aligned} \tag{A6}$$

with a_i, b_i can be written as

$$\begin{aligned} &a_1=k_1,\ b_1=-\{k_1(1+k_0-k_2)+\mathbf{k}_1\cdot(-\mathbf{k}_0+\mathbf{k}_2)\}, \\ &a_2=k_2,\ b_2=-\{k_2(1+k_0-k_1)+\mathbf{k}_2\cdot(-\mathbf{k}_0+\mathbf{k}_1)\}, \\ &a_3=-k_0,\ b_3=\{k_0(1-k_1-k_2)+\mathbf{k}_0\cdot(\mathbf{k}_1+\mathbf{k}_2)\}, \end{aligned} \tag{A7}$$

with k_0, k_1 and k_2 being the energies (in m_0c^2 units) of the incident and two emitted photons respectively, while $\mathbf{k_0}, \mathbf{k_1}$ and $\mathbf{k_2}$ (in m_0c units) are the corresponding momenta.

In a similar way the absorption differential cross section, $\mathrm{d}({}_e\sigma_a)$, representing true absorption of energy from the electromagnetic radiation (gamma rays) is given by the relation:

$$\mathrm{d}({}_e\sigma_a)=(\alpha r_0^2/16\pi^2m_0c^2)(E_1E_2/E_0)(X/T_a), \tag{A8}$$

with

$$T_a=(k_0/(k_0-k_1-k_2))\{1+k_0(1-\cos\theta_2)-k_1(1-\cos\theta_{12})\}. \tag{A9}$$

Thus apart from incident energy parameter, the expressions for $\mathrm{d}({}_e\sigma_s)$ and $\mathrm{d}({}_e\sigma_a)$ are complicated functions of energies and directions of the emitted gamma quanta and their physical contents are difficult to display.

References

[1] F Mandl and T H R Skyrme, *Proc. R. Soc. (London)* **A215**, 497 (1952)
[2] B S Sandhu, M B Saddi, B Singh and B S Ghumman, *Nucl. Instrum. Methods* **B168**, 329 (2000)
[3] B S Sandhu, B Singh and B S Ghumman, *Appl. Radiat. Isot.* **44**, 1367 (1993)
[4] B S Sandhu, B Singh and B S Ghumman, *J. Phys. Soc. Jpn.* **63(9)**, 3243 (1994)
[5] R D Evans, in *Handbuch Der Physik* edited by S Flügge (Springer-Verlag, Berlin, 1958) vol. XXXIV, p. 218
[6] C E Crouthamel, *Applied gamma ray spectrometry* (Pergamon Press, London, 1960)
[7] P Axel, *Rev. Sci. Instrum.* **25**, 39 (1954)
[8] W J Veigele, *At. Data* **5(1)**, 51 (1973)
[9] J H Hubbell, *Radiat. Res.* **70**, 58 (1977)
[10] P E Cavanagh, *Phys. Rev.* **87**, 1131 (1952)
[11] R N Lee, A I Milstein and V M Strakhovenko, *Phys. Rev.* **A58**, 1757 (1998)